Role of multiple minijets in high-energy hadronic reactions

Xin-Nian Wang
Nuclear Science Division, Mailstop 70A-3307, Lawrence Berkeley Laboratory, University of California, Berkeley, California 94720
(Received 30 March 1990)

The multiplicity distributions of charged particles in high-energy hadron collisions including the production of multiple minijets are considered in the framework of the eikonal formalism. Large-multiplicity events at high energies are found to be dominated by the production of many jets with $2 \leq P_T \leq 4$ GeV. The contributions from larger-P_T minijets become prevailing for high-multiplicity fluctuations in narrow rapidity intervals.

I. INTRODUCTION

In high-energy nucleon-nucleon collisions, the production of minijets becomes increasingly important for colliding energies beyond the CERN ISR energy range.[1] Many model calculations indicate that minijets are responsible for the rapid growth of pp and $p\bar{p}$ cross sections,[2,3] the violation of Koba-Nielsen-Olesen (KNO) scaling of multiplicity distributions,[4-8] and the increase of average transverse momentum with charged multiplicity[8-12] at high energies.

Even though minijets are produced in semihard QCD processes, the number of such processes grows with energy with the expectation of multiple-jet production[13] because of the rapid increase in the parton (mainly gluon) distribution at small fractional momentum. In the light of recent experiments at the Fermilab Tevatron collider energy $\sqrt{s} = 1.8$ TeV, in which an event can produce as many as 200 charged particles,[14] it is of interest to know how many jets contribute to such events and what is the important range of their transverse momenta. In particular, what is the balance between the contributions from many jets with $P_T \lesssim$ few GeV and the contributions from a few jets but with larger P_T? By clarifying this problem, we can have a better understanding of the mechanism responsible for KNO scaling violation and the average $\langle p_T \rangle$ increase with multiplicity[12] and increasing energy. The problem is also important for the investigation of the effects of QCD jets on particle production and transverse-energy flow in high-energy heavy-ion collisions. It has been estimated[15] that there could be copious minijet production at the proposed Brookhaven Relativistic Heavy Ion Collider (RHIC) with energy of 100+100 GeV/nucleon.

The focus of this paper is on the contributions of multiple jets to the multiplicity distributions of the produced particles in pp or $p\bar{p}$ collisions. For this purpose we extend the QCD-inspired eikonal formalism[2,10] for pp or $p\bar{p}$ cross sections to take multiple-minijet production into account. In this approach we assume geometrical scaling[16-18] at low energies and extrapolate it to high energies for the soft part of interactions. In the calculation of the total cross section, we find that the parameter for the jet transverse-momentum cutoff must be $P_0 > 1$ GeV in order to reproduce the experimental values of $\sigma_{\rm tot}(s)$. The main reason behind this result is due to the reliability of the perturbative QCD at small P_T. Another reason might be related to the structure function of the proton at small x or shadowing effects[19] of gluons. When the gluon density in a proton is so high at extremely small x, they begin to interact and annihilate with each other, eventually reaching a saturation limit. For small P_0 and extremely large $\sqrt{s}$, the structure function we use now will overestimate the gluon density at around $x_0 = 2P_0/\sqrt{s}$, thus giving too large values to the inclusive jet cross sections. It is estimated[19] that the shadowing effects should be small at presently available energies for $P_0 > 1$ GeV. But when higher-order corrections are taken into account, the situation may change. We assume that the shadowing effect can be neglected for the value of $P_0 = 2$ GeV in the energy range of our discussion.

We limit ourselves to the whole phase space when discussing the total multiplicity distributions. Our main conclusion is that the events of large multiplicity at high energies are mainly from those consisting of many jets with $2 \lesssim P_T \lesssim 4$ GeV. On the average, the effects of jet production depend on the P_T cutoff P_0. With $P_0 = 2$ GeV, jet production can only become dominant above the Tevatron collider energy of 1.8 TeV. The contributions from $P_T > 4$ GeV minijets, which are significantly suppressed for the multiplicity distribution in the whole phase space, can become substantial for a large-multiplicity fluctuation in small rapidity windows.

The production of multiple jets in pp and $p\bar{p}$ collisions has been considered before by some models with Monte Carlo simulation such as the dual parton model,[5] FRITIOF,[7] PYTHIA,[8] and others.[11] However, we treat here the problem consistently in the eikonal formalism. The soft-particle production in this paper is different from previous models. A similar study of the influence of single-minijet production on multiplicity distribution can be found in Ref. 10. In that model the broadening of the multiplicity distribution ceases to increase at sufficiently high energies. However, a peculiar parametrization of the average multiplicity from jet fragmentation has to be introduced in order to account for what should come from multiple minijets.

The remainder of the paper is organized as follows. In

Sec. II we review the QCD-inspired eikonal formulas for pp or $p\bar{p}$ cross sections and the cross sections of multiple-minijet production. The constraint imposed by the total cross section on the soft contribution for different assumptions about the minijet cutoff scale P_0 is discussed in detail. The total multiplicity distributions of nucleon-nucleon collisions including multiple-minijet production are computed in Sec. III. Particle production from jets in restricted rapidity windows is considered in Sec. IV. Conclusions and remarks are given in Sec. V. Throughout this paper the number of jets refers to the number of parton-parton interactions with transverse momentum beyond some minimum scale P_0.

II. CROSS SECTIONS WITH MULTIPLE MINIJETS

A. Eikonal formalism

In the impact-parameter representation of hadron collisions, the eikonal formalism gives[2,10]

$$\frac{d\sigma_{\rm el}}{dt}=\pi\left[\int_0^\infty b\,db(1-e^{-\chi(b,s)})J_0(b\sqrt{-t})\right]^2, \quad (1)$$

$$\sigma_{\rm el}=\pi\int_0^\infty db^2(1-e^{-\chi(b,s)})^2, \quad (2)$$

$$\sigma_{\rm in}=\pi\int_0^\infty db^2(1-e^{-2\chi(b,s)}), \quad (3)$$

$$\sigma_{\rm tot}=2\pi\int_0^\infty db^2(1-e^{-\chi(b,s)}), \quad (4)$$

in the limit that the real part of the scattering amplitude is small and the eikonal function $\chi(b,s)$ is real. In terms of semiclassical probabilistic model, the factor

$$g(b,s)=1-e^{-2\chi(b,s)}, \quad (5)$$

in Eq. (3), usually referred to as the inelasticity function, can be interpreted as the probability for an inelastic event of nucleon-nucleon collisions at impact parameter b, which may be caused by hard, semihard, or soft-parton interactions. While the nonperturbative soft-parton interactions must be treated phenomenologically, perturbative QCD (PQCD) can be used to calculate hard-parton interactions. The boundary between soft phenomenology and PQCD is specified by a transverse-momentum scale P_0 beyond which PQCD is assumed to be reliable. Considerable controversy[2] surrounds the appropriate choice of $P_0\sim 1$–3 GeV. However, we will see that in the eikonal framework, a value below 1 GeV is not compatible with $\sigma_{\rm tot}(s)$. For a given P_0, multiple-minijet production can be assumed to proceed independently until it reaches such high energies that the number of partons at $x_0=2P_0/\sqrt{s}\ll 1$ becomes so large that shadowing becomes important. When shadowing can be neglected, the probability of no jets and j independent jet production in an inelastic event at impact parameter b can be written as

$$g_0(b,s)=(1-e^{-2\chi_s(b,s)})e^{-2\chi_h(b,s)}, \quad (6)$$

$$g_j(b,s)=\frac{[2\chi_h(b,s)]^j}{j!}e^{-2\chi_h(b,s)}, \quad j\geq 1, \quad (7)$$

where $2\chi_h(b,s)$ is the average number of hard-parton interactions at a given b and $\chi_s(b,s)$ is the eikonal function for soft interactions so that $e^{-2\chi_s(b,s)}$ is the probability of no soft interactions. Summing Eqs. (6) and (7) over all values of j leads to

$$\sum_{j=0}^{\infty}g_j(b,s)=1-e^{-2\chi_s(b,s)-2\chi_h(b,s)}. \quad (8)$$

Comparing with Eq. (5), one has

$$\chi(b,s)=\chi_s(b,s)+\chi_h(b,s). \quad (9)$$

If we consider that the parton distribution function is factorizable in longitudinal and transverse directions and that shadowing can be neglected, the average number of hard interactions $2\chi_h(b,s)$ at the impact parameter b is given by

$$\chi_h(b,s)=\tfrac{1}{2}\sigma_{\rm jet}(s)A(b,s), \quad (10)$$

where $A(b,s)$ is the effective partonic overlap function of the nucleons at impact parameter b,

$$A(b,s)=\int d^2b'\rho(b')\rho(|b-b'|), \quad (11)$$

with normalization $\int d^2b\,A(b,s)=1$, and $\sigma_{\rm jet}(s)$ is the PQCD cross section of parton interaction or jet production,[20]

$$\sigma_{\rm jet}(s)=\int_{P_0^2}^{s/4}dP_T^2dy_1dy_2\frac{1}{2}\frac{d\sigma_{\rm jet}}{dP_T^2dy_1dy_2}, \quad (12)$$

$$\frac{d\sigma_{\rm jet}}{dP_T^2dy_1dy_2}=\sum_{a,b}x_1x_2\left[f_a(x_1,P_T^2)f_b(x_2,P_T^2)\frac{d\sigma^{ab}(\hat{s},\hat{t},\hat{u})}{d\hat{t}}+f_b(x_1,P_T^2)f_a(x_2,P_T^2)\frac{d\sigma^{ab}(\hat{s},\hat{u},\hat{t})}{d\hat{t}}\right]\left[1-\frac{\delta_{a,b}}{2}\right], \quad (13)$$

where the summation runs over all parton species, P_0 is the low-P_T cutoff, x_1 and x_2 are the fractions of the momenta of the nucleons the partons carry, which are related to their final rapidities y_1,y_2 and transverse momentum P_T by $x_1=x_T(e^{y_1}+e^{y_2})/2$, $x_2=x_T(e^{-y_1}+e^{-y_2})/2$, and $x_T=2P_T/\sqrt{s}$. The relevant region of x_1 and x_2 is restricted to $x_1<1$, $x_2<1$, and $x_1x_2>4P_T^2/s$. The integration region of y_1 and y_2 in Eq. (12) at fixed P_T is then bounded by

$$\begin{aligned}&-\ln(2/x_T-e^{-y_1})\leq y_2\leq\ln(2/x_T-e^{y_1}),\\ &|y_1|\leq\ln\{1/x_T+[(1/x_T^2-1)]^{1/2}\}.\end{aligned} \quad (14)$$

Some arguments[21] could lead to a modification of the integration region. But the final results are not very different. This is particularly true when we calculate the total inclusive jet cross section which is more dependent on the P_T cutoff. The differential parton cross sections $d\sigma^{ab}/d\hat{t}$ are compiled in Ref. 22. We use the Duke-

Owens[23] parametrization of parton distribution functions with P_T as the hard scale and $\Lambda_{QCD}=200$ MeV. In order to fit the inclusive jet cross section at $y=0$ with the experiments, a K factor of 2.5 has to be used in the calculations.[24]

For $P_0>1$ GeV, $\sigma_{jet}(s)$ is found to be very small when $\sqrt{s}\lesssim 20$ GeV. Therefore, only $\chi_s(b,s)$ in Eq. (9) is important for small $\sqrt{s}$. The low-energy data of diffractive nucleon-nucleon scatterings exhibit a number of geometrical scaling properties[25] in the range $10<\sqrt{s}<100$ GeV, e.g., $\sigma_{el}/\sigma_{tot}\cong 0.175$ and $B/\sigma_{tot}\cong 0.3$, where B is the slope of the diffractive peak of the differential elastic cross section. This suggests a geometrical scaling form[16,17] for the eikonal function $\chi_s(b,s)$, i.e.; it is only a function of $\xi=b/b_0(s)$, where

$$\pi b_0^2(s)\equiv\sigma_0(s)\ , \tag{15}$$

which is proportional to $\sigma_{tot}(s)$. One can assume[26] that $\chi_s(b,s)$ is proportional to the nucleon overlap function $A(b,s)$, which we will take as given by Eq. (11) with $\rho(b,s)$ being the Fourier transform of a dipole form factor $(1-t/\mu^2)^{-2}$. Thus, similarly to the definition of $\chi_h(b,s)$, we have

$$\chi_s(b,s)=\frac{1}{2}\sigma_s(s)A(b,s)=\frac{\sigma_s(s)}{2\sigma_0(s)}\chi_0(\xi)\ , \tag{16}$$

$$\chi_0(\xi)=\frac{\mu_0^2}{96}(\mu_0\xi)^3K_3(\mu_0\xi),\quad \xi=\frac{b}{b_0(s)}\ , \tag{17}$$

where $\mu_0=b_0\mu$ is considered as an adjustable parameter, $\sigma_0(s)$ is a measure of the geometrical size of the nucleons, and $\sigma_s(s)$ can be regarded as the cross section for the soft-parton interactions. Note that $\int_0^\infty d\xi^2\chi_0(\xi)=1$. In the CERN ISR energy range, geometrical scaling means that, as $\sqrt{s}$ increases, a hadron increases in size, while its opaqueness at a fixed impact parameter b also increases in such a way that $\chi_s(b,s)$ depends only on the scaled variable ξ. Therefore, in order to have geometrical scaling properties, we simply set $\sigma_s(s)=2\sigma_0(s)$ so that $\chi_s(b,s)=\chi_0(\xi)$. One can readily check that Eqs. (1)–(4) give constant σ_{el}/σ_{tot} and B/σ_{tot}. We find that $\mu_0=3.9$ can reproduce the experimental data well, which corresponds to a value of $\mu=0.8$ GeV for $\sigma_0=28.5$ mb. We will extrapolate these properties to high energies for the soft part of the interactions. However, when discussing the constraint on P_0, we will relax this assumption on geometrical scaling for the soft interactions. In that case, $\sigma_s(s)$ and $\sigma_0(s)$ are only related via Eq. (16).

Assuming the same geometrical distribution for both soft and hard overlap functions, we get

$$\chi_h(\xi,s)\equiv\frac{\sigma_{jet}(s)}{2\sigma_0(s)}\chi_0(\xi)\ ,$$
$$\chi_s(\xi,s)\equiv\frac{\sigma_s(s)}{2\sigma_0(s)}\chi_0(\xi)\ , \tag{18}$$

$$\chi(\xi,s)\equiv\frac{1}{2\sigma_0(s)}[\sigma_s(s)+\sigma_{jet}(s)]\chi_0(\xi)\ . \tag{19}$$

We note that $\chi(\xi,s)$ is a function not only of ξ, but also of $\sqrt{s}$, because of the $\sqrt{s}$ dependence of the jet cross section $\sigma_{jet}(s)$. Geometrical scaling at low energies implies, on the other hand, that $\chi_s(\xi,s)=\chi_0(\xi)$, is only a function of ξ. Therefore, the geometrical scaling is broken at high energies by the introduction of the nonvanishing $\sigma_{jet}(s)$ of jet production.

Before we go on, let us rewrite the cross sections of nucleon-nucleon collisions in Eqs. (2)–(4) as

$$\sigma_{el}=\sigma_0(s)\int_0^\infty d\xi^2(1-e^{-\chi(\xi,s)})^2\ , \tag{20}$$

$$\sigma_{in}=\sigma_0(s)\int_0^\infty d\xi^2(1-e^{-2\chi(\xi,s)})\ , \tag{21}$$

$$\sigma_{tot}=2\sigma_0(s)\int_0^\infty d\xi^2(1-e^{-\chi(\xi,s)})\ . \tag{22}$$

Integrating Eqs. (6) and (7) over the impact parameter and then dividing them by $\sigma_{in}(s)$, we have the total probability for no and j number of jets in an inelastic event:

$$G_0=\frac{\sigma_0(s)}{\sigma_{in}(s)}\int_0^\infty d\xi^2(1-e^{-2\chi_s(\xi,s)})e^{-2\chi_h(\xi,s)}\ , \tag{23}$$

$$G_j=\frac{\sigma_0(s)}{\sigma_{in}(s)}\int_0^\infty d\xi^2\frac{[2\chi_h(\xi,s)]^j}{j!}e^{-2\chi_h(\xi,s)}\ . \tag{24}$$

The calculation of these cross sections requires specifying $\sigma_s(s)$ with a corresponding value of P_0. In the ISR energy range $10<\sqrt{s}<70$ GeV, where only soft-parton interactions are important, $\sigma_s(s)$ is fixed by the data on $\sigma_{tot}(s)$ directly. In and above the CERN S$p\bar{p}$S energy range $\sqrt{s}\geq 200$ GeV, we fix $\sigma_s(s)$ at a value of 57 mb with $P_0=2$ GeV in order to fit the data of the cross sections. Between the two regions $70<\sqrt{s}<200$ GeV, we simply use a smooth extrapolation for $\sigma_s(s)$. The results are shown in Figs. 1 and 2. Note that in Fig. 1(a) the calculated $\sigma_{tot}(s)$ (solid line) goes through ISR,[27] S$p\bar{p}$S,[28,29] Tevatron,[30] as well as the cosmic-ray[31,32] data points, while $\sigma_{jet}(s)$ (dashed line) increases rapidly with ln$s$. For illustration, we also give $\sigma_s(s)=2\sigma_0(s)$ (dot-dashed line)

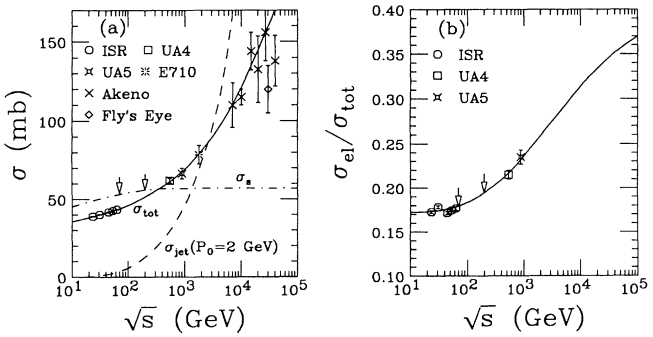

FIG. 1. (a) Calculated cross sections vs $\sqrt{s}$. The solid line is for σ_{tot}, dashed line for σ_{jet} with $P_0=2$ GeV, and dot-dashed line for the corresponding $\sigma_s=2\sigma_0$. In the ISR energy range (Ref. 27), σ_s is fitted by the data on σ_{tot}. Above $\sqrt{s}=200$ GeV, σ_s is fixed at a constant value of 57 mb. In between, as indicated by arrows, a smooth extrapolation is used. (b) σ_{el}/σ_{tot} vs $\sqrt{s}$. The data are from Refs. 17 and 28–30.

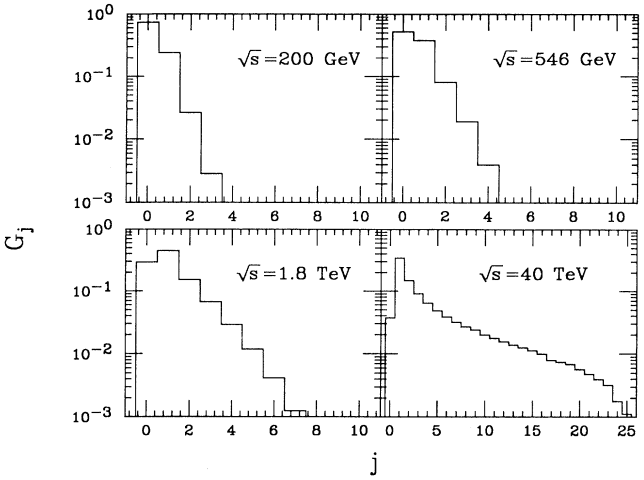

FIG. 2. Probability distributions G_j of the production of j number of minijets at $\sqrt{s}=200$ GeV 546 GeV, 1.8 TeV, and 40 TeV.

in Fig. 1(a), which is almost constant, even in the ISR energy range. In Fig. 1(b) we plot $\sigma_{\rm el}/\sigma_{\rm tot}$ as a function of $\sqrt{s}$. The data are from Refs. 28, 29, and 17. It is clearly shown that geometrical scaling is violated above ISR energies. Figure 2 gives our calculated probability distributions of multiple-minijet production at four different energies. We see that as the energy increases, the probability of multiple-minijet production increases considerably.

B. Constraints on low-P_T cutoff P_0

We emphasize that the value of $P_0=2$ GeV used in the above calculation is a phenomenological parameter. In order that the model have predicative power, P_0 should not depend on $\sqrt{s}$. However, its value is subject to considerable controversy.[2] The problem arises from the boundary between soft and hard processes specified by P_0. The question of how hard an interaction should be in order to be counted as a hard or semihard collision and what should be included in the soft-parton interactions can only be answered phenomenologically. Since we require a fit to $\sigma_{\rm tot}(s)$, the choice of $\sigma_s(s)$ and P_0 must be correlated. The inclusive cross section of parton interactions $\sigma_{\rm incl}(s)$ can be decomposed into a soft $\sigma_s(s)$ and hard part $\sigma_{\rm jet}(s)$:

$$\sigma_{\rm incl}(s)\equiv\sigma_s(s)+\sigma_{\rm jet}(s) = \int_0^{P_0^2} dP_T^2 \frac{d\sigma_{\rm incl}}{dP_T^2} + \int_{P_0^2}^{s/4} dP_T^2 \frac{d\sigma_{\rm jet}}{dP_T^2} , \quad (25)$$

where $d\sigma_{\rm jet}/dP_T^2$ is given by PQCD. Of course, no quantitative theory for the low-P_T region exists, and we must treat the region phenomenologically. With a smaller P_0, more events are counted as hard collisions. Hence $\sigma_s(s)$ would be smaller and vice versa. Obviously, many choices of P_0 and $\sigma_s(s)$ can give the same total cross section $\sigma_{\rm tot}(s)$. The only restriction is that the sum $\sigma_s(s)+\sigma_{\rm jet}(s)$ must have the right value to give the right energy dependence of the total cross section $\sigma_{\rm tot}(s)$. Since $\sigma_{\rm jet}(s)$ increases with decreasing P_0 and $\sigma_s(s)$ is non-negative, P_0 must be bounded from below by the experimental data on the total cross section $\sigma_{\rm tot}(s)$. We find that this lower limit in our model is $P_0=1.2$ GeV. For P_0 smaller than 1.2 GeV, the inclusive jet cross section at high energies is overestimated and the resultant $\sigma_{\rm tot}(s)$ can never fit the data. If one insists that the noncalculable soft-parton interactions never vanish, the actual limit on P_0 would be higher than 1.2 GeV. In addition, one must keep in mind that the lowest P_0 is also bounded by the relevant $Q_0=P_0$ in the evolution of the parton distribution function.

In Fig. 3 we give up geometrical scaling for the soft interactions by choosing a constant σ_0 with a value of 28.5 mb and illustrate the correlation between $\sigma_s(s)$ and P_0 for two values of $P_0=1.2$ and 3 GeV. In both cases, $\sigma_s(s)$ is fitted to give the right total cross section $\sigma_{\rm tot}(s)$. Contrary to $P_0=2$ GeV, $\sigma_s(s)$ in both cases must vary with energy in order to give the right total cross section $\sigma_{\rm tot}(s)$. Especially for $P_0<2$ GeV (e.g., 1.2 GeV), the decrease of $\sigma_s(s)$ with s due to the rapid increase of $\sigma_{\rm jet}(s)$ is very hard to understand. Moreover, Duke-Owens parametrization of the parton distribution function, which is only valid for $P_0\geq 2$ GeV, had already underestimated the parton density at small x for $P_0<2$ GeV. Therefore, it is natural for us, based on the geometrical scaling approach, to choose the value $P_0=2$ GeV with a constant $\sigma_s(s)=2\sigma_0(s)=57$ mb, which reproduces $\sigma_{\rm tot}(s)$ well. The parameters also reproduce the right geometrical scaling violation, i.e., the increase of $\sigma_{\rm el}(s)/\sigma_{\rm tot}(s)$ with $\sqrt{s}$ as shown in Fig. 1(b).

III. MULTIPLICITY DISTRIBUTION WITH MULTIPLE MINIJETS

A. Soft and hard production

In order to evaluate the total multiplicity distributions, we must again differentiate the contributions from soft

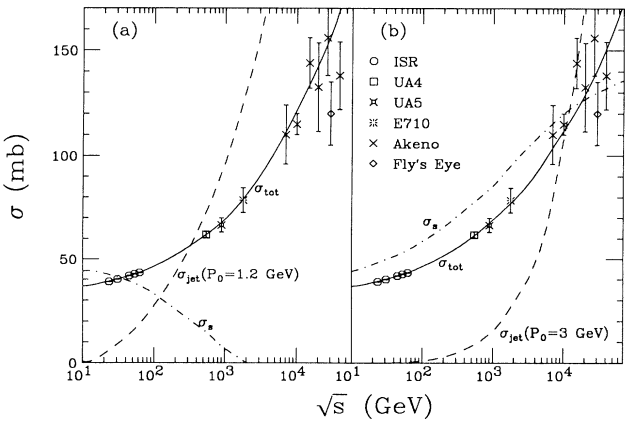

FIG. 3. Same as Fig. 1(a), except that it is calculated with constant σ_0 and varying $\sigma_s(s)$ for (a) $P_0=1.2$ GeV and (b) $P_0=3.0$ GeV.

and hard processes. We use the geometrical branching model[18] (GBM) in this paper for the soft-particle production and the empirical results from e^+e^- data for the jet fragmentation. Since GBM does not specify the distributions in momentum space, we consider primarily the multiplicity distributions in the whole phase space.

GBM assumes Furry branching as the basic process of particle production in soft hadronic collisions at each impact parameter. It has been shown[18] that the multiplicity distribution

$$P_n^s=\frac{\int_0^\infty d\xi^2(1-e^{-2\chi_s(\xi,s)})F_n^{k(\xi)}(w)}{\int_0^\infty d\xi^2(1-e^{-2\chi_s(\xi,s)})} \tag{26}$$

possesses KNO scaling and the calculated results fit the experimental data well in the ISR energy range. When extended to the cases of hadron-nucleus and nucleus-nucleus collisions[33] at low energies, it also reproduces the experimental results well. In Eq. (26), $F_n^{k(\xi)}(w)$ is the Furry distribution

$$F_n^{k(\xi)}(w)=\frac{\Gamma(n)}{\Gamma(k(\xi))\Gamma(n-k(\xi)-1)}\times\left[\frac{1}{w}\right]^{k(\xi)}\left[1-\frac{1}{w}\right]^{n-k(\xi)}, \tag{27}$$

where

$$k(\xi)\equiv k(s,\xi)=\bar{k}(s)h_s(\xi)\ , \tag{28}$$

$$\bar{n}(s,\xi)=\bar{n}_s(s)h_s(\xi)\ , \tag{29}$$

$$h_s(\xi)=\frac{\chi_s(\xi,s)}{1-e^{-2\chi_s(\xi,s)}}\int_0^\infty d\xi^2(1-e^{-2\chi_s(\xi,s)})\ , \tag{30}$$

and $w=\bar{n}_s(s)/\bar{k}(s)=1+0.104\bar{n}_s(s)$. Detailed derivation of these equations can be found in Ref. 18. Note that the parameter here is slightly different from Ref. 18 because the eikonal functions $\chi_s(\xi,s)$ are different. For the average multiplicity from the soft-particle production $\bar{n}_s(s)$, we parametrize the low-energy data as

$$\bar{n}_s(s)=2.3\ln s-5.6\ , \tag{31}$$

and extrapolate it to high energies.

The jets produced in nucleon-nucleon collisions can be either quark or gluon jets, though the gluon-gluon scatterings are dominant among other semihard subprocesses because of the rapid increase of the gluon distribution function at small x. The solution to the evolution equations of fragmentation functions[34] gives a gluon jet $\frac{9}{4}$ times the average multiplicity of a quark jet. However, studies in both $p\bar{p}$ and e^+e^- experiments[35,36] show little difference between the two, especially at low energies. Since we are only interested in minijets, we will approximate both gluon and quark jets with an effective one. When we are only concerned with the multiplicity distribution in the whole phase space, the particles from initial- and final-state radiation will also be included in the jets, though the rapidity distributions are very different between the particles from jets and those from the initial- and final-state radiation. Thus the effective jet will follow the properties of the ones in e^+e^-, e.g., the multiplicity and rapidity distributions of the charge particles. The energy dependence of the average multiplicity will be the same, and only the overall coefficient is different.

We take a Poisson form, which fits the e^+e^- data well, as the multiplicity distribution for the charged particles from jet fragmentation:

$$h_n(\bar{n}_{\rm jet})=\frac{(\bar{n}_{\rm jet})^n}{n!}e^{-\bar{n}_{\rm jet}}\ , \tag{32}$$

where $\bar{n}_{\rm jet}(\hat{s})$ is the average multiplicity which varies with the center-of-mass energy $\hat{s}$ of the jets. It is known[37] that the average multiplicity of e^+e^- can be fitted by $2.18s^{1/4}$. Therefore, we assume that for the jets in nucleon-nucleon collisions,

$$\bar{n}_{\rm jet}(\hat{s})=(1+c)2.18\hat{s}^{1/4}\ , \tag{33}$$

where $c=0.26$ is to be found late when fitting the total charged multiplicity. The reason why $c>0$ is due to initial- and final-state radiation as well as the difference between gluon and quark jets. This is well demonstrated by the Monte Carlo model PYTHIA.[8] Experimentally, the so-called pedestal effect caused by the radiation has also been seen in the UA1 data.[1] After averaging over the rapidities and transverse momentum of the jets, the multiplicity distribution of the charged particles from a single hard process is then

$$H_n(s)=\frac{1}{\sigma_{\rm jet}}\int_{P_0^2}^{s/4}dP_T^2dy_1dy_2h_n(\bar{n}_{\rm jet})\frac{1}{2}\frac{d\sigma_{\rm jet}}{dP_T^2dy_1dy_2}\ , \tag{34}$$

where $\sigma_{\rm jet}$ is given by Eq. (12). The average multiplicity from a hard collision is

$$\langle n\rangle_{\rm jet}=\frac{1}{\sigma_{\rm jet}}\int_{P_0^2}^{s/4}dP_T^2dy_1dy_2\bar{n}_{\rm jet}(\hat{s})\frac{1}{2}\frac{d\sigma_{\rm jet}}{dP_T^2dy_1dy_2}\ . \tag{35}$$

B. Multiplicity distribution

By Eqs. (23) and (24), the total multiplicity distribution can be written as

$$P_n=\sum_{j=0}^\infty G_jP_n^j\ , \tag{36}$$

$$G_0P_n^0=\frac{\sigma_0(s)}{\sigma_{\rm in}(s)}\int_0^\infty d\xi^2(1-e^{-2\chi_s(\xi,s)})e^{-2\chi_h(\xi,s)}F_n^{k(\xi)}(w)\ , \tag{37}$$

$$G_jP_n^j=\frac{\sigma_0(s)}{\sigma_{\rm in}(s)}\int_0^\infty d\xi^2\frac{[2\chi_h(\xi,s)]^j}{j!}e^{-2\chi_h(\xi,s)}\Phi_n^j(\xi,s)\ , \tag{38}$$

where

$$\Phi_n^j(\xi,s)=\sum_{l,n_1,\ldots,n_j}\delta_{n,l+\Sigma_{n_i}}F_l^{k(\xi)}(w)\prod_{i=1}^j H_{n_i}(s)\ , \tag{39}$$

$H_n(s)$ given in Eq. (34) is the multiplicity distribution for a single hard collision, and $F_l^{k(\xi)}$ given in Eq. (27) is that for soft interactions. The main assumption behind these formulas is that the center-of-mass energy $\hat{s}=x_1x_2s$ of each semihard collision is small on the average compared to the total energy s and all the semihard subprocesses can be treated independently.

From Eqs. (36)–(39), (27)–(30) and (35), we can obtain the total averaged multiplicity as

$$\langle n\rangle(s)=\frac{1}{\sigma_{\rm in}}\left[\sigma_0(s)\int_0^\infty d\xi^2(1-e^{-2\chi(\xi,s)})\times h_s(\xi)\bar{n}_s(s)+\sigma_{\rm jet}\langle n\rangle_{\rm jet}\right]. \quad (40)$$

By fitting the total averaged multiplicity $\langle n\rangle$ with the experimental value at one high energy, we can fix the value of $c=0.26$ in Eq. (33). Using the parameter thus determined, we can calculate the total averaged multiplicity for all other energies. The result is shown in Fig. 4 with data from Fermilab, Serpukhov, ISR,[38] and UA5 (Refs. 29 and 40) experiments. The energy dependence of $\langle n\rangle(s)$ is well reproduced. In the same figure we also show the contributions from the hard and soft processes. The average number of particles from soft production is still proportional to the logarithm of $\sqrt{s}$, while that of jets is increasing much faster and finally becomes dominant at higher energies. However, that only happens for energy above $\sqrt{s}=4$ TeV. The rapid increase of the contribution to the total multiplicity from the jets is due not only to the increase of the center-of-mass energy of the jets, but also the increase in the average number of jets $\sigma_{\rm jet}(s)/\sigma_{\rm in}(s)$ produced.

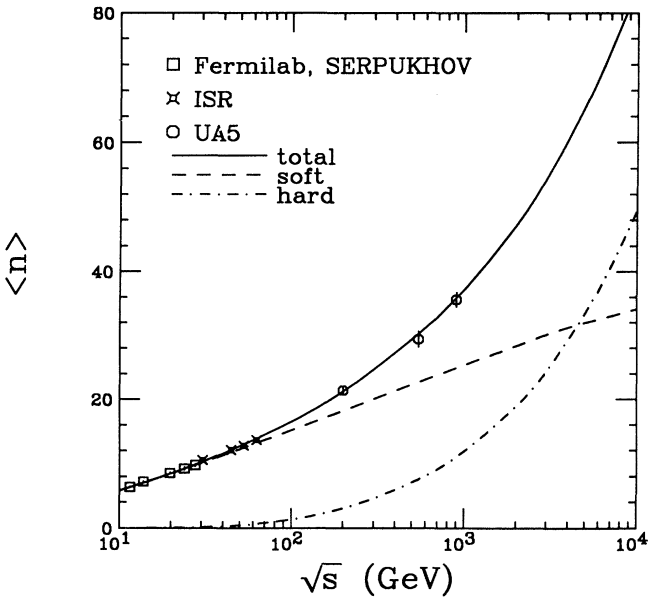

FIG. 4. Average charged multiplicities in pp or $p\bar{p}$ collisions. The solid line is the total average multiplicity. The dashed line is the contribution from soft production, and the dot-dashed line is the contribution from jet production. The data are from Refs. 38–40.

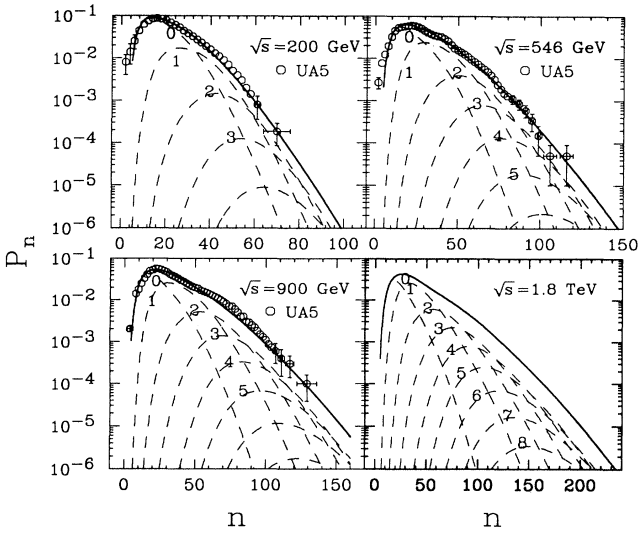

FIG. 5. Calculated multiplicity distributions for the charged particles in nucleon-nucleon collisions at $\sqrt{s}=200$ GeV, 546 GeV, 900 GeV, and 1.8 TeV. The data are from Refs. 40 and 39. The dashed lines are the contributions to the solid ones from events which consist of the soft component and the production of $j=0,1,2,\ldots$ number of minijets.

The calculated multiplicity distributions are given in Fig. 5 as solid lines along with the available experimental data.[38,40] Our calculations, including the effects of multiple minijets, reproduce well the energy dependence of the data. Also shown in this figure as dashed lines are the contributions from the events which have j hard collisions with $P_T\geq P_0$ as obtained via Eqs. (37)–(39). Note that each j component always includes a soft part. It is clear that the events at the tails of the multiplicity distributions are mainly those with multiple-jet production. To show the violation of KNO scaling, we plot the multiplicity distribution in KNO form in Fig. 6 at three different energies and the normalized moments of the distributions as functions of $\sqrt{s}$ in Fig. 7. We can see that the broadening of the KNO distribution or the KNO scaling violation is due to the production of multiple minijets. The tendency becomes stronger with increasing energy.

To compare our results with standard Monte Carlo models, we have used PYTHIA to calculate the same multiplicity distributions. In PYTHIA a double Gaussian has been used for matter distribution in a proton. Instead of a P_T cutoff, a shift of P_T^2 to $P_T^2+P_{T0}^2$ is made in the differential cross section of the hard parton-parton interactions. In Fig. 8 we show both the result of PYTHIA with $P_{T0}=1.9$ GeV and ours at $\sqrt{s}=546$ GeV. Both of the two are consistent with experiment, although there are some discrepancies for PYTHIA at the peak. Detailed calculation reveals that the average multiplicity from the soft-parton interaction in our model is a little larger and the corresponding distribution is also wider than that in PYTHIA at high energies. The effect of initial- and final-state radiations plays an important role in both cases. In our case, setting $c=0$ gives results similar to those of

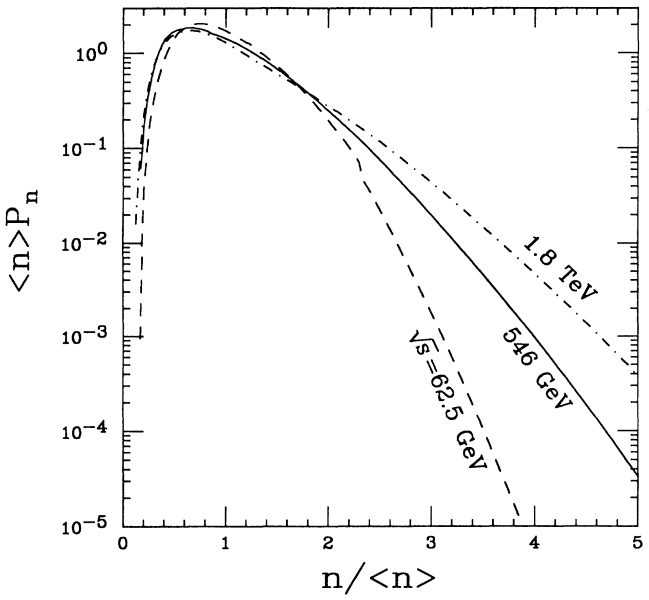

FIG. 6. KNO plot of multiplicity distributions of produced particles in nucleon-nucleon collisions at $\sqrt{s}=62.5$ GeV, 546 GeV, and 1.8 TeV.

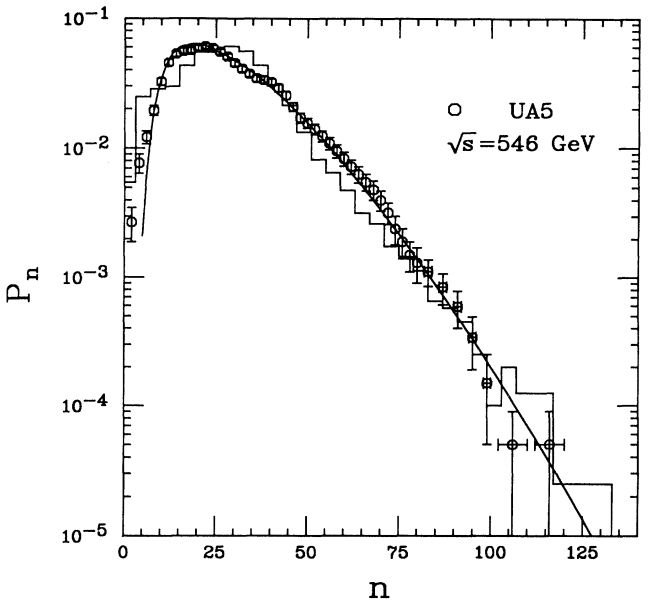

FIG. 8. Multiplicity distribution of charged particles in nucleon-nucleon collisions at $\sqrt{s}=546$ GeV. The solid curve is our calculation, and the histogram is that of PYTHIA. The data are from Ref. 39.

PYTHIA with the initial- and final-state radiations turned off.

IV. PARTICLE PRODUCTION FROM MINIJETS

Having seen that large multiplicity events in nucleon-nucleon collisions contain many minijets, we investigate now what are the typical transverse momenta of these jets at different multiplicities. Furthermore, we generalize here to the case with different rapidity cuts. Therefore, the rapidity distribution of the particles from the jet fragmentation need to be determined. Similar to Eq. (33), we assume that the rapidity density along the jet's axis is also proportional to that of e^+e^-. A good parametrization of e^+e^- data[37] is given by

$$\frac{dn_{\rm jet}}{dy}=\frac{\bar{n}_0(\hat{s})}{1+e^{3(|y|-y_{\rm max})}}\ , \tag{41}$$

where

$$\bar{n}_0(\hat{s})=(1+c)(0.743+0.238\ln\hat{s}) \tag{42}$$

is the height of the central plateau and $y_{\rm max}$ is the half-width of the plateau determined by $\bar{n}_{\rm jet}(\hat{s})=\int_{-\infty}^{\infty}(dn_{\rm jet}/dy)dy$, or

$$y_{\rm max}=\tfrac{1}{3}\ln(e^{3\bar{n}_{\rm jet}(\hat{s})/2\bar{n}_0(\hat{s})}-1)\ . \tag{43}$$

Suppose that a pair of jets in a nucleon-nucleon collision have rapidities y_1 and y_2. By a Lorentz boost with $y_b=(y_1+y_2)/2$ with respect to the original frame, we consider the situation in the center-of-mass frame of two colliding partons. The jets then have rapidities $\pm y^*=\pm(y_1-y_2)/2$, and a particle with a rapidity y' along the jet's axis has

$$\sinh y=\frac{\sinh y'\sinh y^*}{(\cosh^2 y^*+\sinh^2 y')^{1/2}}\ , \tag{44}$$

where the intrinsic transverse momentum in the jet fragmentation has been ignored. Note that $|y|\le|y^*|$. Therefore, the averaged number of particles which fall into a rapidity window y_c is then

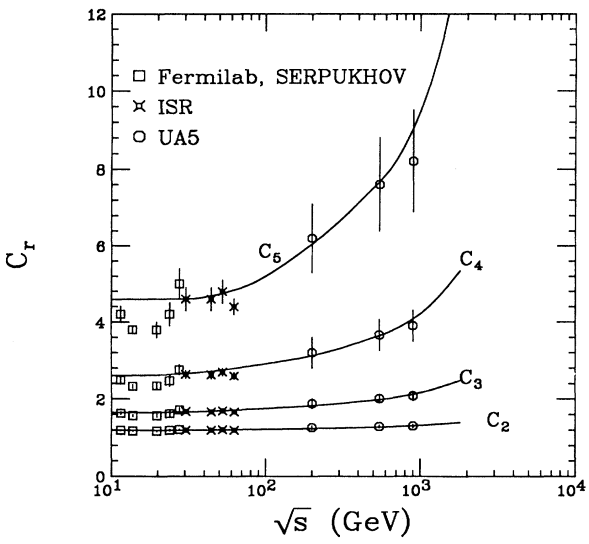

FIG. 7. Normalized moments of multiplicity distributions in nucleon-nucleon collisions vs $\sqrt{s}$. The data are from Refs. 38–40.

$$\bar{n}_{\rm jet}(y_1,y_2,y_c,\hat{s})=\int_{y_1'}^{y_2'} dy' \frac{dn_{\rm jet}}{dy'} , \tag{45}$$

where $dn_{\rm jet}/dy'$ is given by Eq. (41) and

$$\sinh y_1' = \frac{-\sinh(y_c+y_b)\cosh y^*}{[\sinh^2 y^* - \sinh^2(y_c+y_b)]^{1/2}} , \tag{46}$$

$$\sinh y_2' = \frac{\sinh(y_c-y_b)\cosh y^*}{[\sinh^2 y^* - \sinh^2(y_c-y_b)]^{1/2}} , \tag{47}$$

which are obtained from Eq. (44) by restricting

$$|y+y_b| \le y_c . \tag{48}$$

Note that when $|y_c-|y^*|| \le |y_b|$, all particles from jet fragmentation will fall into the window. Especially when $y^*=0$, all particles will have rapidity y_b. When $y_c \to \infty$ or $y_c \gg \ln(\sqrt{s}/P_0)$, $\bar{n}_{\rm jet}(y_1,y_2,y_c,\hat{s})$ becomes $\bar{n}_{\rm jet}(\hat{s})$ as given in Eq. (33). Substituting $\bar{n}_{\rm jet}(\hat{s})$ by $\bar{n}_{\rm jet}(y_1,y_2,y_c,\hat{s})$ in Eq. (34), we can calculate the charged-multiplicity distribution $H_n(s)$ of the particles from the jet fragmentation of a hard collision within the window y_c. The results are shown in Figs. 9 and 10.

In Fig. 9 we show $H_n(s)$ (solid lines) for two different energies, but with no rapidity cut. Even though the Poisson distribution in Eq. (32) is narrow, it becomes very broad after being smeared over the transverse momentum and rapidities of the jets, because of the variation of the virtuality of the subprocess. In this plot we also give the contributions from different P_T regions (dashed, dot-dashed, and dash-dash-dotted lines). The contributions from large transverse momentum jets with $P_T \ge 6$ GeV is significantly suppressed, especially at large multiplicities. The dominant contributions come from those jets with small P_T which characterizes minijets or semihard collisions. This is because jet production is dominated by collinear events. Even though their P_T are small, these

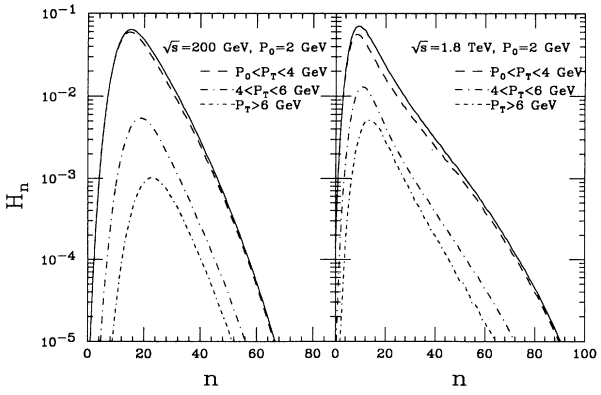

FIG. 9. Multiplicity distributions (solid lines) of particles from an inclusive jet production with low-P_T cutoff $P_0=2$ GeV in nucleon-nucleon collisions at $\sqrt{s}=200$ GeV and 1.8 GeV. The dashed, dot-dashed, and dash-dash-dotted lines are the contributions to the solid ones from regions of $P_0<P_T<4$ GeV, $4<P_T<6$ GeV, and $P_T>6$ GeV, respectively.

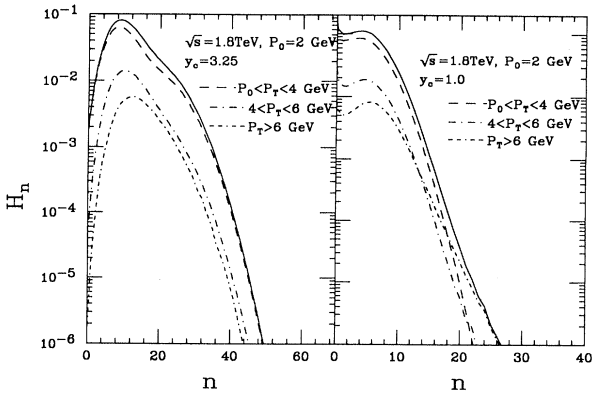

FIG. 10. Same as Fig. 9, except for $\sqrt{s}=1.8$ TeV with rapidity cuts $y_c=3.25$ and 1.

jets could have a comparatively large center-of-mass energy $\hat{s}$ and can therefore produce a large number of particles by independent fragmentation. In order to increase the contributions from large P_T jets to the distribution at large multiplicities, one has to limit oneself to a very small rapidity window in the central rapidity region. In this way the events with large n can only come from those jets with large P_T. Indeed, in Fig. 10, where we show the distributions $H_n(s)$ with two rapidity cuts at $\sqrt{s}=1.8$ TeV, contributions from large P_T jets are increasing with smaller y_c. When $y_c=1$, for example, the contributions from $P_T \ge 6$ GeV are dominant at large multiplicities. Therefore, triggering on high multiplicities in restricted rapidity windows intrinsically biases the events toward larger P_T multiple minijets.

V. CONCLUSIONS AND REMARKS

In the framework of eikonal formalism, we have extended the QCD-inspired model[2] to describe multiple independent production of minijets. We have shown in this paper that the violation of KNO scaling of multiplicity distribution in high-energy hadron-hadron collisions can be understood as due to multiple-minijet production with $P_0 \approx 2$ GeV. The contributions to particle production from fragmentation of the minijet increase with the colliding energy $\sqrt{s}$ and become dominant at energies around the Superconducting Super Collider energy. We showed that most of the contributions to the multiplicity distribution from jets with $P_T \le 4$ GeV. However, in narrow rapidity windows an increase in the contributions from the production of jets with large P_T is correlated with high multiplicities.

The separation of hard and soft subprocesses must be introduced to include a PQCD calculable part in addition to a phenomenological nonperturbative soft part. The transverse-momentum cutoff P_0 for jet production is the scale beyond which semihard interactions may be treated perturbatively. Any value of $P_0 > 1$ GeV may do, but phenomenologically the value of 2 GeV leads to a con-

stant $\sigma_s = 2\sigma_0$ needed for reproducing the experimental values of $\sigma_{\rm tot}$ and $\sigma_{\rm el}/\sigma_{\rm tot}$. For $P_0 < 1.2$ GeV, an unphysical $\sigma_s(s)$ is required.

The advantage of the present calculation over standard Monte Carlo simulations is its analytic simplicity. In addition, the model provides a direct means to gauge the uncertainties associated with soft processes and to ascertain the relative importance of multiple-minijet production. The problem is furthermore treated consistently in the framework of the eikonal approximation, and geometrical scaling is preserved at low energies.

ACKNOWLEDGMENTS

The author is grateful to M. Gyulassy and R. C. Hwa for their inspiration, encouragement, and help discussions. He would also like to thank T. Sjöstrand for providing the Monte Carlo program PYTHIA and many helpful communications. This work was supported by the Director, Office of Energy Research, Division of Nuclear Physics of the Office of High Energy and Nuclear Physics of the U.S. Department of Energy under Contract No. DE-AC03-76SF00098.

[1]C. Albajar *et al.*, Nucl Phys. **B309**, 405 (1988); A. Norton, in *Multiparticle Production,* proceedings of the Shandong Workshop, Jinan, China, 1987, edited by R. C. Hwa and Q. B. Xie (World Scientific, Singapore, 1988), p. 87.

[2]T. K. Gaisser and F. Halzen, Phys. Rev. Lett. **54**, 1754 (1985); P. l'Heureux *et al.*, Phys. Rev. D **32**, 1681 (1985); G. Pancheri and Y. N. Srivastava, Phys. Lett. B **182**, 199 (1986); L. Durand and H. Pi, Phys. Rev. Lett. **58**, 303 (1987); J. Dias de Deus and J. Kwiecinski, Phys. Lett. B **196**, 537 (1987).

[3]P. Carruthers and I. Sarcevic, Phys. Rev. D **40**, 1446 (1989).

[4]Z. Koba, H. N. Nielsen, and P. Olesen, Nucl. Phys. **B40**, 317 (1972).

[5]A. Capella and J. Tran Thanh Van, Z. Phys. C **23**, 165 (1984).

[6]A. D. Martin and C. J. Maxwell, Phys. Lett. B **172**, 248 (1986), Z. Phys. C **34**, 71 (1987).

[7]B. Andersson, G. Gustafson, and B. Nilsson-Almqvsit, Nucl. Phys. **B281**, 289 (1987).

[8]T. Sjöstrand and M. van Zijl, Phys. Rev. D **36**, 2019 (1987).

[9]G. Pancheri and Y. N. Srivastava, in *Multiparticle Production* (Ref. 1).

[10]R. C. Hwa, Phys. Rev. D **37**, 1830 (1988); W. R. Chen and R. C. Hwa, *ibid.* **39**, 179 (1989).

[11]T. K. Gaisser and Todor Stanev, Bartol report, 1988 (unpublished).

[12]X. N. Wang and R. C. Hwa, Phys. Rev. D **39**, 187 (1989).

[13]B. Humpert, Phys. Lett. **131B**, 461 (1983); N. Paver and D. Treleani, *ibid.* **146B**, 252 (1984).

[14]T. Alexopoulos *et al.*, Nucl. Phys. A **498**, 181c (1989).

[15]K. Kajantie, P. V. Landshoff, and J. Lindfors, Phys. Rev. Lett. **59**, 2527 (1987); K. J. Eskola, K. Kajantie, and J. Lindfors, Nucl. Phys. **B323**, 37 (1989).

[16]J. Dias de Deus, Nucl. Phys. **B59**, 231 (1973); **B252**, 369 (1985).

[17]U. Amaldi and K. R. Schubert, Nucl. Phys. **B166**, 301 (1980).

[18]W. R. Chen and R. C. Hwa, Phys. Rev. D **36**, 760 (1987); W. R. Chen, R. C. Hwa, and X. N. Wang, *ibid.* **38**, 3394 (1988).

[19]A. H. Mueller, in *Proceedings of the Oregon Meeting,* Annual Meeting of the Division of Particles and Fields of the APS, Eugene, Oregon, 1985, edited by R. C. Hwa (World Scientific, Singapore, 1986), p. 634; A. H. Mueller and J. Qui, Nucl. Phys. **B268**, 427 (1986).

[20]E. Eichten, I. Hinchliffe, and C. Quigg, Rev. Mod. Phys. **56**, 579 (1984).

[21]See Durand and Pi (Ref. 2); L. Durand and H. Pi, Phys. Rev. D **38**, 78 (1988).

[22]E. Learder and E. Predazzi, *An Introduction to Gauge Theories and the New Physics* (Cambridge University Press, Cambridge, England, 1982), pp. 462–468; B. L. Cambridge and C. J. Maxwell, Nucl. Phys. **B239**, 429 (1984).

[23]D. W. Duke and J. F. Owens, Phys. Rev. D **30**, 50 (1984).

[24]G. Arnison *et al.*, Phys. Lett. B **172**, 461 (1986); C. Albajar *et al.*, Nucl. Phys. **B309**, 405 (1986).

[25]For a review of the scaling properties, see articles in *Elastic and Diffractive Scatterings,* edited by B. Nicolescu and J. Tran Than Van (Editions Frontières, Gif-sur-Yvette, France, 1985).

[26]T. T. Chou and C. N. Yang, Phys. Rev. Lett. **20**, 1213 (1968); Phys. Rev. **170**, 1591 (1968).

[27]N. Amos *et al.*, Phys. Lett. **120B**, 461 (1983); **128B**, 343 (1983).

[28]UA4 Collaboration, M. Bozzo *et al.*, Phys. Lett. **147B**, 392 (1984).

[29]UA5 Collaboration, P. Carlson, in *Proceedings of the Oregon Meeting* (Ref. 19), p. 615.

[30]N. Amos *et al.*, Phys. Rev. Lett. **63**, 2784 (1989).

[31]R. M. Baltrusaitis *et al.*, Phys. Rev. Lett. **52**, 1380 (1984).

[32]T. Hara *et al.*, Phys. Rev. Lett. **50**, 2058 (1983). The *pp* cross sections converted from *p*-air data are taken from L. Durand and H. Pi, Phys. Rev. Lett. **58**, 303 (1987).

[33]R. C. Hwa and X. N. Wang, Phys. Rev. D **39**, 2561 (1989); X. N. Wang and R. C. Hwa, *ibid.* **39**, 2573 (1989); R. C. Hwa and X. N. Wang, *ibid.* **42**, 1459 (1990).

[34]A. H. Mueller, Nucl. Phys. **B241**, 141 (1984); E. D. Malaza and B. R. Webber, Phys. Lett. **145B**, 501 (1984).

[35]UA2 Collaboration, P. Bagnaia *et al.*, Z. Phys. C **20**, 117 (1983).

[36]M. Derrick *et al.*, Phys. Lett. **165B**, 449 (1985).

[37]TASSO Collaboration, M. Althof *et al.*, Z. Phys. C **22**, 307 (1984).

[38]UA5 Collaboration, G. J. Alner *et al.*, Phys. Lett. **160B**, 199 (1985).

[39]UA5 Collaboration, G. J. Alner *et al.*, Phys. Rep. **154**, 247 (1987).

[40]UA5 Collaboration, R. E. Ansorge *et al.*, Z. Phys. C **43**, 357 (1989).